The Effect of Oxygen on the Kinetics and Particle Size Distribution in Vinyl Chloride Emulsion Polymerization

Costas Kiparissides,* Dimitris S. Achilias, and Costas E. Frantzikinakis

Department of Chemical Engineering and Chemical Process Engineering Research Institute, Aristotle University of Thessaloniki, P.O. Box 472, Thessaloniki, Greece 540 06

A comprehensive mathematical model is developed to quantify the effect of the oxygen concentration on the polymerization rate and particle size distribution in an unseeded vinyl chloride batch emulsion polymerization reactor. Particle formation is assumed to proceed by both the homogeneous and micellar nucleation mechanisms. Dynamic species mass balances are derived to follow the evolution of the polymerization rate and particle size distribution (PSD) in the batch reactor. It is shown that, at low initial oxygen concentrations, the polymerization rate increases with the oxygen concentration. On the other hand, the average latex particle size exhibits a U-shaped behavior with respect to the initial oxygen concentration. The experimental observations on the polymerization rate and the average particle size are explained by the combined role of oxygen as an inhibitor and a radical generator through the formation and subsequent decomposition of vinyl polyperoxides. The predictive capabilities of the present model are demonstrated through the successful simulation of experimental data on monomer conversion and PSD obtained from an industrial pilot-plant batch PVC reactor operated with various initial oxygen and initiator concentrations.

Introduction

The inhibitive role of molecular oxygen on the free-radical emulsion polymerization of vinyl monomers is well-known.[1] Oxygen is capable of reacting with initiator primary radicals and oligomers in the aqueous phase to produce vinyl polyperoxides. Vinyl polyperoxides (VPPs) are alternating copolymers of vinyl monomers with oxygen, which, because of their current resurgence in various potential applications (such as special fuels, initiators, and curatives in coating and molding), have been established as an important class of polymers.[2] Under certain experimental conditions, the vinyl polyperoxides can decompose into radicals, which are capable of initiating new polymer chains, and small molecules (e.g., HCl), which can alter the ionic strength of the reaction medium. Thus, by careful control of the residual oxygen in the initial degassing stage of the reactor, it is possible to utilize the in situ formation of vinyl polyperoxides to increase the emulsion polymerization rate without increasing the amount of chemical initiators.[3]

The effect of residual oxygen on the emulsion polymerization reaction of vinyl chloride has been qualitatively discussed by Zilbermann.[4] However, no quantitative kinetic models have been developed to describe the effect of the residual oxygen concentration on the polymerization rate and the particle size distribution. Recent experimental results obtained from a pilot-plant batch vinyl chloride (VC) emulsion polymerization reactor have shown that the reaction rate, as well as the average particle size, can either increase or decrease depending on the initial oxygen concentration. As a result, the development of a comprehensive mathematical model to predict the effect of the oxygen concentration on the reaction kinetics and particle size distribution is of profound importance to the vinyl chloride emulsion polymerization industry.

The mathematical modeling of emulsion polymerization reactors has been the subject of numerous publications.[5−12] The complex physicochemical phenomena taking place in the reactor constitute the main reason for the difficulties associated with the development of a comprehensive mathematical model. Among the other modeling difficulties, the particle nucleation rate is particularly difficult to quantify, because there are a number of physically reasonable contributions to it that cannot easily be assessed. When the polymerization is carried out under emulsifier-free conditions, the particle size distribution of the latex will be strongly influenced by the ionic strength of the aqueous phase, which affects the colloidal stability of the precursor particles.[13−16] At least two main theories (i.e., the micellar and the homogeneous) have been proposed to describe particle nucleation phenomena in emulsion polymerization reactions. According to the micellar nucleation theory, new particles are formed upon the entry of free radicals into micelles. On the other hand, in the homogeneous coagulative nucleation, particle formation is effected by the precipitation and subsequent coagulation of growing oligomers in the aqueous phase. Thus, the particle size distribution in an emulsion polymerization reactor will largely depend on the particle nucleation and coagulation mechanisms, which are, in turn, influenced by the polymerization temperature, the emulsifier concentration, the initial initiator concentration, and the ionic strength of the medium, as well as the presence of seed particles.

The mathematical modeling of batch VC emulsion polymerization reactors has been addressed in several publications.[17−19] However, no paper addresses the

* Corresponding author. Tel.: +30310 99 6211. Fax: +30310 99 6198. E-mail: cypress@alexandros.cperi.certh.gr.

10.1021/ie010928f CCC: $22.00
Published on Web 06/01/2002

Table 1. Emulsion Polymerization Kinetic Mechanism

description	reaction
initiator decomposition	$I \xrightarrow{k_I} 2I^{\bullet}$
propagation in the aqueous phase	$R^{\bullet}_{1,w} + M_w \xrightarrow{k_{p11}} R^{\bullet}_{1,w}$
propagation in the polymer phase	$R^{\bullet}_{1,p} + M_p \xrightarrow{k_{p11}} R^{\bullet}_{1,p}$
chain transfer to monomer in the polymer phase	$R^{\bullet}_{1,p} + M_p \xrightarrow{k_f} R^{\bullet}_{1,p} + P_p$
termination by combination in the aqueous (j = w) and the polymer phase (j = p)	$R^{\bullet}_{1,j} + R^{\bullet}_{1,j} \xrightarrow{k_{tj11}} P_j$
termination by disproportionation in the queous (j = w) and the polymer phase (j = p)	$R^{\bullet}_{1,j} + R^{\bullet}_{1,j} \xrightarrow{k_{tj11}} P_j + P_j$

effect of oxygen on the reaction kinetics, particle nucleation, and particle stability. In the present study, a comprehensive mathematical model is proposed to quantify the effect of the oxygen concentration on the kinetics and PSD developments in a VC emulsion polymerization batch reactor. Additional elementary reactions are included in the classical kinetic mechanism to take into account the combined role of oxygen as a radical generator or/and an inhibitor. The formation of vinyl polyperoxides (VPPs) is assumed to occur via the copolymerization of VCM with oxygen.[20] VPPs can subsequently decompose into free radicals, which are capable of initiating new polymer chains, and small molecules (such as HCl in the case of VC polymerization), which can alter the ionic strength of the aqueous medium and, thus, the particle stability and particle aggregation rate.[21] Particle formation is assumed to occur by both the homogeneous and micellar nucleation mechanisms. Detailed species mass balances are derived to follow the time evolution of the monomer conversion, total number of particles, number-average molecular weight, and particle size distribution in a batch reactor.

In what follows, the fundamental mathematical model developments are presented, including the kinetic mechanism, the dynamic molar species balances in the aqueous and polymer phases, and a population balance equation describing the time evolution of the particle size distribution in a batch emulsion polymerization reactor. Finally, model predictions are compared with experimental data on monomer conversion and average particle size obtained from an industrial pilot-plant batch reactor.

Mathematical Model Developments

Kinetic Mechanism. The kinetic mechanism of the emulsion polymerization of vinyl monomers commonly includes the elementary reactions shown in Table 1. The symbols I, $I^{\bullet}$, and M_j denote the initiator, the primary initiator radicals, and the monomer in the aqueous (j = w) and polymer phases (j = p), respectively. P_j denotes the "dead" polymer chains.

To account for the effect of oxygen on the emulsion polymerization kinetics, the following additional elementary reactions, occurring in the aqueous phase, are considered:[20,4]

Reaction of oxygen with a growing radical of type 1

$$R^{\bullet}_{1,w} + O_2 \xrightarrow{k_{p12}} R^{\bullet}_{2,w} \quad (1)$$

Reaction of monomer with a growing radical of type 2

$$R^{\bullet}_{2,w} + M_w \xrightarrow{k_{p21}} R^{\bullet}_{1,w} \quad (2)$$

Formation of vinyl polyperoxides oligomers

$$R^{\bullet}_{2,w} + R^{\bullet}_{1,w} \xrightarrow{k_{tw12}} P_w \quad (3)$$

Subsequent decomposition of the vinyl polyperoxides (VPPs) results in the formation of free radicals and HCl according to the reaction

$$P_w \xrightarrow{k_{dVPP}} R^{\bullet}_{1,w} + n\mathrm{HCl} \quad (4)$$

where $R^{\bullet}_{1,w}$ identifies the type of "live" copolymer chains, that is, polymer chains ending in a VC monomer unit (i = 1) or in an oxygen unit (i = 2).

It should be noted that the effects of oxygen and VPP are considered only in the aqueous phase.

Dynamic Molar Species Balances. Using the above kinetic mechanism, the following set of ordinary differential equations can be derived to describe the conservation of the various molar species in the aqueous, polymer, and emulsion phases in a batch reactor:[7]

Initiator concentration in the aqueous phase

$$\frac{d[I_w]}{dt} = -\frac{[I_w]}{V_w}\frac{dV_w}{dt} - k_I[I_w] \quad (5)$$

Initially added electrolyte concentration

$$\frac{d[Y_w]}{dt} = -\frac{[Y_w]}{V_w}\frac{dV_w}{dt} \quad (6)$$

Monomer concentration in the emulsion phase

$$\frac{d[M_e]}{dt} = -\frac{[M_e]}{V_e}\frac{dV_e}{dt} - R_{pe} \quad (7)$$

Monomer concentration in the "dead" polymer phase

$$\frac{d[M_{qe}]}{dt} = -\frac{[M_{qe}]}{V_e}\frac{dV_e}{dt} + R_{pp} \quad (8)$$

Concentration of polymer chains in the emulsion phase

$$\frac{d[P_e]}{dt} = -\frac{[P_e]}{V_e}\frac{dV_e}{dt} + R_{ew} + k_f[R^{\bullet}_{1,p}][M_p]\frac{V_p}{V_e} \quad (9)$$

Added surfactant concentration in the emulsion phase

$$\frac{d[S_e]}{dt} = -\frac{[S_e]}{V_e}\frac{dV_e}{dt} \quad (10)$$

Oxygen concentration in the aqueous phase

$$\frac{d[O_2]}{dt} = -\frac{[O_2]}{V_w}\frac{dV_w}{dt} - k_{p12}[R^{\bullet}_{1,w}][O_2] \quad (11)$$

VPP concentration in the aqueous phase:

$$\frac{d[VPP]}{dt} = -\frac{[VPP]}{V_w}\frac{dV_w}{dt} + k_{tw12}[R^{\bullet}_{1,w}][R^{\bullet}_{2,w}] - k_{dVPP}[VPP] \quad (12)$$

HCl concentration in the aqueous phase

$$\frac{d[HCl]}{dt} = -\frac{[HCl]}{V_w}\frac{dV_w}{dt} + nk_{dVPP}[VPP] \quad (13)$$

The time variation of the total emulsion volume, V_e, as well as of the polymer, V_p, and aqueous, V_w, phases is given by the differential equations

$$\frac{dV_e}{dt} = \left(\frac{1}{\rho_p} - \frac{1}{\rho_m}\right)MW_m R_{pe} V_e \quad (14)$$

$$\frac{dV_p}{dt} = MW_m R_{pp}\frac{V_e}{\varphi_p \rho_p} - \frac{V_p}{\varphi_p}\frac{d\varphi_p}{dt} \quad (15)$$

$$\frac{dV_w}{dt} = \frac{F_w}{C_{ww}} - \frac{Q_e V_w}{V_e} \quad (16)$$

Note that the volume of the aqueous phase in the batch reactor remains constant. Accordingly, the volume of the separate monomer phase, V_m, can be obtained by subtracting the volumes of the aqueous and polymer phases from the total emulsion volume

$$V_m = V_e - V_p - V_w \quad (17)$$

The total monomer consumption rate in the emulsion phase, R_{pe}, is given by the sum of the monomer consumption rates in the polymer particles, R_{pp}, and in the aqueous phase, R_{pw}

$$R_{pe} = R_{pp} + R_{pw} \quad (18)$$

$$R_{pp} = (k_{p11} + k_f)[R^{\bullet}_{1,p}][M_p]V_p/V_e \quad (19)$$

$$R_{pw} = \{(k_{p11} + k_f)[R^{\bullet}_{1,w}] + k_{p21}[R^{\bullet}_{2,w}]\}[M_w]V_w/V_e \quad (20)$$

For the calculation of the polymerization rates R_{pp} and R_{pw}, one needs to know the monomer concentrations in the aqueous phase, $[M_w]$, and in the polymer particles, $[M_p]$. Moreover, the pseudo-steady-state concentrations of live radicals $[R^{\bullet}_{1,w}]$, $[R^{\bullet}_{2,w}]$, and $[R^{\bullet}_{1,p}]$ must be available.

Calculation of the Equilibrium Monomer Distribution. One of the major issues in the development of a comprehensive mathematical model for an emulsion polymerization reactor is the calculation of the equilibrium monomer distribution in the various phases. In the VCM emulsion polymerization, one can identify three different phases, namely, the aqueous phase, the monomer droplets, and the polymer particles.

The equilibrium monomer distribution in the polymer particles, $[M_p]$, in the aqueous phase, $[M_w]$, and in the monomer droplets, $[M_d]$, can be calculated in terms of the monomer partition coefficients and the saturated monomer concentrations. The saturated monomer concentration in the aqueous phase, $[M_w]_{sat}$, can be expressed in terms of the monomer solubility, K_{sol} (grams of monomer/grams of water) and the water density

$$[M_w]_{sat} = K_{sol}\rho_w/MW_m \quad (21)$$

On the other hand, the saturated monomer concentration in the polymer phase, $[M_p]_{sat}$, can be calculated in terms of the critical monomer conversion, x_c, at which the separate monomer droplet phase disappears and the densities of the monomer and the polymer

$$[M_p]_{sat} = (1 - x_c)\rho_m/\left[\left(1 - x_c + x_c\frac{\rho_m}{\rho_p}\right)MW_m\right] \quad (22)$$

Accordingly, one can define the monomer partition coefficients between the aqueous phase and the polymer particles, K_{mwp}, and between the monomer droplets and the polymer particles, K_{mdp}, as

$$K_{mwp} = [M_w]_{sat}/[M_p]_{sat} \quad (23)$$

$$K_{mdp} = [M_d]/[M_p] = K_{mdw}K_{mwp} = \frac{(\rho_m/MW_m)}{[M_w]_{sat}}K_{mwp} \quad (24)$$

Thus, the monomer concentration in the polymer particles can be calculated from the expressions

$$[M_p] = [M_p]_{sat} \qquad x \le x_c$$

$$[M_p] = (1 - x)\rho_m/\left[\left(1 - x + x\frac{\rho_m}{\rho_q}\right)MW_m\right] \qquad x > x_c \quad (25a)$$

and the monomer concentration in the aqueous phase can be determined according to

$$[M_w] = K_{mwp}[M_p] \quad (25b)$$

Finally, the monomer volume fraction, φ_m, and the corresponding polymer volume fraction, φ_p, in the swollen polymer particles are given by

$$\varphi_m = [M_p]MW_m/\rho_m$$
$$\varphi_p = 1 - \varphi_m \quad (26)$$

Calculation of the Aqueous- and Polymer-Phase Radical Concentrations. The dynamic molar balance for the total concentration of live copolymer chains in the aqueous phase, $[R^{\bullet}_w]$, is given by the differential equation

$$\frac{1}{V_w}\frac{d([R^{\bullet}_w]V_w)}{dt} = R_{Iw} + R_d - R_{ew} - R_{emw} - R_{tw} \quad (27)$$

where the terms R_{Iw}, R_d, R_{ew}, R_{emw}, and R_{tw} denote the net rate of primary radical production via the decomposition of initiator(s) and vinyl polyperoxides, the rate of radical desorption from latex particles, the rate of radical entry into particles, the rate of radical entry into micelles, and the rate of radical termination in the aqueous phase, respectively.

Assuming that the quasi-steady-state approximation (QSSA) for the live radical chains in the aqueous phase holds true, eq 27 becomes

$$R_{Iw} + R_d - R_{ew} - R_{emw} - R_{tw} = 0 \quad (28)$$

According to the long-chain hypothesis (LCH), the concentrations of live copolymer chains of types $R^{\bullet}_{1,w}$ and $R^{\bullet}_{2,w}$ will satisfy the equations

$$k_{p12}[R^{\bullet}_{1,w}][O_2] = k_{p21}[R^{\bullet}_{2,w}][M_w] \quad (29)$$

$$[R^{\bullet}_{w}] = [R^{\bullet}_{1,w}] + [R^{\bullet}_{2,w}] \quad (30)$$

Equation 29 implies that the number of times a VC monomer unit is followed by an oxygen unit will be, either exactly or plus/minus one, equal to the number of times an oxygen unit is followed by a VC monomer unit. Thus, from eqs 28−30, the concentrations of $[R^{\bullet}_{1,w}]$ and $[R^{\bullet}_{2,w}]$ can be calculated in terms of the rates R_{Iw}, R_d, R_{ew}, R_{emw}, and R_{tw}, defined as described in the following sections.

Primary Radical Production Rate. The net primary radical production rate can be expressed as

$$R_{Iw} = 2k_I[I_w] + k_{dVPP}[VPP] \quad (31)$$

where k_I and k_{dVPP} denote the initiator and VPP decomposition rate constants, respectively.

Radical Desorption Rate. The net radical desorption rate from the latex particles can be obtained by integrating the radical desorption rate from a single particle with respect to the total particle size distribution (PSD)

$$R_d = \int_{r_0}^{r_{max}} k_d(r)\, \bar{n}(r) \left(\frac{f(r)}{N_A}\right)\left(\frac{V_e}{V_w}\right) dr \quad (32)$$

where $f(r)\, dr$ denotes the number of particles in the size range between r and $r + dr$ per unit volume of emulsion. Following the developments of Ugelstad and Hansen,[22] the radical desorption coefficient, $k_d(r)$, of a particle of radius r can be expressed in terms of the propagation, k_p, and transfer-to-monomer, k_f, rate constants; the monomer concentration in the polymer particles, $[M_p]$; the average number of radicals per particle, $\bar{n}(r)$; and the desorption rate constant, $k_0(r)$ as

$$k_d(r)^{-1} = (k_f[M_p])^{-1} + (k_0(r)k_f[M_p]/[k_p[M_p] + k_0(r)\, \bar{n}(r)])^{-1} \quad (33)$$

Accordingly, the desorption rate constant can be calculated in terms of the diffusion coefficients of live polymer chains in the aqueous phase, D_w, and in the polymer particles, D_p[23]

$$k_0(r) = 3D_wK_{mwp}/[r^2(1 + D_wK_{mwp}/2D_p)] \quad (34)$$

Rate of Radical Entry into Particles. The total rate of radical entry into the polymer particles is defined as

$$R_{ew} = \int_{r_0}^{r_{max}} \sum_{i=1}^{2} k_{ei}[R^{\bullet}_{i,w}] \left(\frac{f(r)}{N_A}\right)\left(\frac{V_w}{V_e}\right) dr \quad (35)$$

where k_{ei} is the rate coefficient for radical entry into a particle of radius r[24]

$$k_{ei}(r) = 4\pi r N_A D_w U/W(r_1,r_2) \quad (36)$$

U is a radical reversibility parameter, accounting for the reversible diffusion of live oligomeric polymer chains into the polymer particles. $W(r_1,r_2)$ is the Fuchs' stability ratio, accounting for the electrostatic repulsion forces between oligomeric radicals of radius r_1 and electrically charged particles of radius r_2 (see eq 62).

Rate of Radical Entry into Micelles. The rate of radical entry into the micelles can be expressed as

$$R_{emw} = 4\pi r_m{}^2 \sum_{i=1}^{2} k_{mi}[R^{\bullet}_{i,w}] N_A [S_{mw}] \quad (37)$$

where r_m and $[S_{mw}]$ denote the radius and concentration of micelles, respectively.

The concentration of micelles, $[S_{mw}]$, can be calculated from a surfactant surface coverage balance[25]

$$[S_{mw}] = \left([S_w] - [S_{CMC}] - \frac{4\pi r^2 N_e}{N_A(V_w/V_e)a'_S}\right)\frac{a_m}{4\pi r_m{}^2} \quad (38)$$

where $[S_w]$ and $[S_{CMC}]$ are the total surfactant concentration and the critical micelle concentration, respectively. The third term on the RHS of eq 38 accounts for the surfactant concentration adsorbed by the latex particles. Finally, a_m and a'_s denote the surface areas occupied by a surfactant molecule in a micelle and in a latex particle, respectively. Note that, in eq 38, the amount of surfactant adsorbed by the monomer droplets is assumed to be negligible.

Radical Termination Rate. The rate of radical termination in the aqueous phase, R_{tw}, can be expressed as

$$R_{tw} = \sum_{i=1}^{2}\sum_{j=1}^{2} (k_{twij}[R^{\bullet}_{i,w}][R^{\bullet}_{j,w}]) \left(\frac{V_w}{V_e}\right) \quad (39)$$

The total concentration of radicals in the latex particles $[R^{\bullet}_{1,p}]$ is determined by integrating the average number of radicals per particle, $\bar{n}(r)$, with respect to the total variation in particle size

$$[R^{\bullet}_{1,p}] = \int_{r_0}^{r_{max}} \bar{n}(r) \left(\frac{f(r)}{N_A}\right)\left(\frac{V_e}{V_p}\right) dr \quad (40)$$

The average number of radicals per particle, $\bar{n}(r)$, is given by the Stockmayer−O'Toole solution to the Smith−Ewart recursion relation

$$\bar{n}(r) = \frac{\xi(r)\, I_{\nu(r)}[\xi(r)]}{4I_{\nu(r)-1}[\xi(r)]} \quad (41)$$

The order, ν, and the argument, ξ, of the modified Bessel function $I_\nu(\xi)$ in eq 41 are defined by the equations

$$\xi = [8\rho(r)/c_t(r)]^{1/2}$$
$$\nu = k_d(r)/c_t(r) \quad (42)$$

where ρ and c_t denote the first-order kinetic rate constants for radical entry into the particles and bimolecular radical termination, respectively. They can be calculated according to[7,26]

$$\rho(r) = \rho_T + \left(\sum_{i=1}^{2} k_{ei}(r)[R^{\bullet}_{i,w}]\right)\frac{V_w}{V_e} + k_d(r)\, \bar{n}(r) \quad (43)$$

$$c_t(r) = 3k_t/(8\pi r^3 N_A) \quad (44)$$

Diffusion-Controlled Phenomena. It is important to mention that, in addition to the conventional chemical kinetics, physical transport phenomena related to the diffusion of various chemically reactive species play a significant role in free-radical polymerizations. Reac-

tions that are influenced by diffusion phenomena include termination of live macroradicals, growth of live polymer chains, and chemical initiation reactions. Diffusion-controlled termination, propagation, and initiation reactions have been related to the well-known phenomena of the gel effect, the glass effect, and the cage effect, respectively. Following the developments of Kiparissides et al.,[27] the termination and propagation rate constants can be expressed in terms of a reaction-limited term and a diffusion-controlled one. The latter depends on the molecular diffusion coefficient of the corresponding species (i.e., polymer chains, monomer) and an effective reaction radius.

Diffusion-Controlled Termination Rate Constant. On the basis of the above modeling approach,[27] the termination rate constant can be expressed as

$$k_t = k_{td} + k_{t,res} \tag{45}$$

where k_{td} and $k_{t,res}$ denote the diffusion-controlled termination rate constant between two live polymer chains in the polymer phase and the so-called "residual termination" rate constant, respectively.

Accordingly, k_{td} can be expressed in terms of an intrinsic termination rate constant, k_{t0}, which is equal to the termination rate constant of live polymer chains in the aqueous phase, plus a diffusion-controlled term

$$\frac{1}{k_{td}} = \frac{1}{k_{t0}} + \frac{r_t^2}{3}\frac{[R^\bullet_{1,p}]}{D_p} \tag{46}$$

where r_t is an effective radius for the termination of live polymer chains given by

$$r_t = \{\ln(1000\tau^3/N_A[R^\bullet_{1,p}]\pi^{3/2})\}^{1/2} \quad \text{where} \quad \tau = \left(\frac{3}{2j_c\delta_d^2}\right)^{1/2} \tag{47}$$

δ_d and j_c are the average root-mean-square end-to-end distance of a polymer chain and the entaglement spacing between polymer chains, respectively.[27] D_p is the polymer self-diffusion coefficient and is calculated from the extended free-volume theory of Vrentas and Duda[28] as

$$D_p = \frac{D_{p0}}{M_w^2}\exp\left(-\gamma\frac{\omega_m\hat{V}^*_m + \omega_p\hat{V}^*_p\xi}{\xi\hat{V}_f}\right) \tag{48}$$

where

$$\xi = \frac{\hat{V}^*_m MW_m}{\hat{V}^*_p MW_p} \quad \text{and} \quad \hat{V}_f = \omega_m\hat{V}^*_m V_{fm} + \omega_p\hat{V}^*_p V_{fp} \tag{49}$$

According to eq 46, at very high monomer conversions, the self-diffusion coefficient of the polymer chains becomes very small, resulting in an unrealistically low value of k_{td}. The reason is that eq 46 does not account for the mobility of live polymer chains caused by the monomer propagation reaction. This phenomenon is known as residual termination. Several models have been proposed for the calculation of the residual termination rate constant $k_{t,res}$.[28] These models assume that $k_{t,res}$ is proportional to the frequency of monomer addition to the radical chain end

$$k_{t,res} = Ak_p[M_e] = Ak_p[M_e]_0(1-x) \tag{50}$$

According to the volume-swept-out model,[28] the proportionality rate constant A, is written as

$$A = \pi\delta_d^3 j_c N_A \tag{51}$$

Diffusion-Controlled Propagation Rate Constant. Accordingly, k_p can be expressed in terms of an intrinsic propagation rate constant k_{p0} (i.e., the propagation rate constant in the aqueous phase) and a diffusion-controlled term accounting for diffusional limitations of the propagation reaction[27]

$$\frac{1}{k_p} = \frac{1}{k_{p0}} + \frac{1}{4\pi r_M N_A D_m} \tag{52}$$

In eq 52, r_M denotes the radius of a monomer molecule. The monomer diffusion coefficient, D_m, is calculated from the extended free-volume theory of Vrentas and Duds[28] as

$$D_m = D_{m0}\exp\left(-\gamma\frac{\omega_m\hat{V}^*_m + \omega_p\hat{V}^*_p\xi}{\hat{V}_f}\right) \tag{53}$$

All symbols used in the preceding equations are explained in the Nomenclature section. All kinetic and transport parameters appearing in eqs 45−53 have clear physical meanings and can be calculated from tabulated data available in the open literature (see Table 3).

Particle Population Balance. In Figure 1, the main steps involved in the formation, growth, and coagulation of latex particles in the VC emulsion polymerization are summarized. On the basis of the proposed particle nucleation mechanism, a general population balance equation can be derived to describe the evolution of the particle size distribution in a batch reactor[29]

$$\frac{\partial n(V,t)}{\partial t} + \frac{\partial[G_p n(V,t)]}{\partial V} = \frac{1}{2}\int_{V_0}^{V-V_0}\beta(V-U,U)\,n(V-U,t)\,n(U,t)\,dU - \int_{V_0}^{V_{max}}\beta(V,U)\,n(V,t)\,n(U,t)\,dU + \delta(V-V_0)R_{pg} \tag{54}$$

where $n(V,t)\,dV$ denotes the number of particles in the size range from V to $V + dV$ at time t per unit volume of the reaction medium. Equation 54 expresses the change in the number volume density function $n(V,t)$ with respect to time (first term) and particle volume (second term). G_p, R_{pg}, and β denote the rate of particle growth due to polymerization, the rate of generation of new particles of volume V_0, and the rate constant for coagulation between two electrically charged colloidal particles, respectively.

The rate of growth of a particle of radius r is given by[7]

$$G_p = \bar{n}(r)\left(\frac{MW_m[M_p]k_{p11}}{N_A\varphi_p\rho_p}\right)\tanh\left(\frac{r}{r_{FH}}\right) \tag{55}$$

Because new particles can be formed by both the homogeneous and the micellar nucleation mechanisms, the overall particle generation rate, R_{pg}, is equal to the

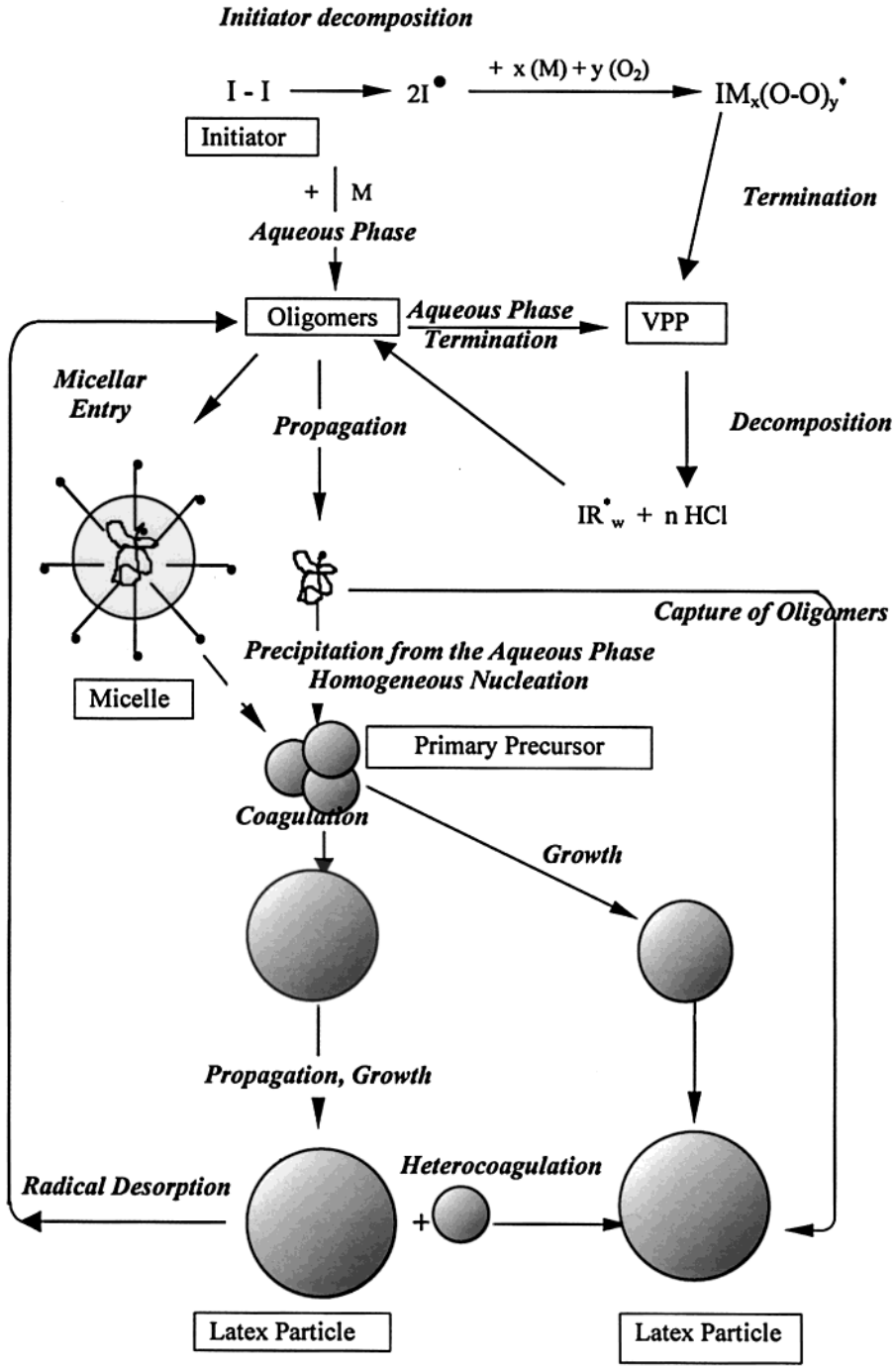

Figure 1. Schematic representation of the mechanism of the particle nucleation and growth mechanisms.

sum of the respective homogeneous and micellar particle nucleation rates

$$R_{pg} = R_{pgh} + R_{pgm} \tag{56}$$

The homogeneous particle nucleation rate is given by the equation[26]

$$R_{pgh} = R_{iw}N_A/\left(1 + \frac{R_{ew} + R_{tw}}{R'_{pw}}\right)^{j_{cr}-1} \tag{57}$$

where j_{cr} denotes the critical degree of polymerization above which live polymer chains formed in the aqueous phase will precipitate to form new primary particles (see also Figure 1)

$$j_{cr} = \frac{V_0\rho_p N_A}{MW_m} \quad \text{where} \quad V_0 = {}^4/_3\pi r_0{}^3 \tag{58}$$

Note that, for the sake of simplicity, eq 57 was employed to calculate the homogeneous nucleation rate of precursor particles instead of the more elaborate model of Casey et al.[30]

The propagation rate in the aqueous phase, R'_{pw}, is given by

$$R'_{pw} = \sum_{i=1}^{2} k_{pi1}[R^{\bullet}_{i,w}][M_w]\left(\frac{V_p}{V_e}\right) + k_{p12}[R^{\bullet}_{1,w}][O_2]\left(\frac{V_p}{V_e}\right) \tag{59}$$

Finally, the micellar particle nucleation rate can be calculated in terms of the rate of radical entry into

micelles, R_{emw}

$$R_{pgm} = R_{emw} V_w / V_e \tag{60}$$

Particle Coagulation Rate Constant. The coagulation rate constant, $\beta(r_i,r_j)$, between two electrically charged colloidal particles is given by the Fuchs modification of the extended Smoluchowski coagulation equation

$$\beta(r_i,r_j) = \beta_{ij} = \frac{2}{3}\frac{kT}{\mu}\frac{(r_i + r_j)^2}{r_i r_j}\frac{1}{W(r_i,r_j)} \tag{61}$$

where k, T, μ, and $W_{ij} = W(r_i,r_j)$ denote the Boltzmann constant, the reaction temperature, the viscosity of the aqueous phase, and the stability ratio, respectively. r_i and r_j are the radii of the ith and jth particles, respectively. The stability ratio depends on the interaction potential V_{max} according to

$$W(r_i,r_j) = W_{ij} \approx (r_i + r_j)\int_0^\infty \frac{1}{h^2}\exp\left(\frac{V_{max}}{kT}\right) dh \tag{62a}$$

For the calculation of the stability ratio, the following approximation was employed[31]

$$W_{ij} \approx \frac{r_i + r_j}{4\kappa r_i r_j}\exp\left(\frac{V_{max}}{kT}\right) \tag{62b}$$

where κ is the reciprocal Debye length and V_{max} is the maximum value of the total interaction potential energy. The reciprocal Debye length, κ, is defined as

$$\kappa = (8\pi {e_L}^2 N_A I_e/\epsilon kT)^{1/2} \tag{63}$$

Assuming that the symmetry of the initiator molecule (i.e., potassium persulfate) is 1:2 and that of the added electrolyte (i.e., sodium chloride) is 1:1, the total ionic strength, I_e, of the medium is given by

$$I_e = 1/2\sum_i {z_i}^2 M_i = 3[I_w] + [Y_w] + [HCl] \tag{64}$$

According to the proposed kinetic mechanism of vinyl polyperoxide formation (see eqs 1−3), hydrogen chloride is produced via the decomposition of the VPPs (see eq 4). As a result, the total ionic strength of the aqueous medium will increase, and thus, the inverse Debye length and the coagulation rate constant will also increase (see eqs 61 and 62).

The maximum value of the total interaction energy, V_{max}, was calculated by eq 65, which was applied over the entire range of variation of the particle radius[17]

$$\frac{V_{max}}{kT} = 8 \times 10^{10}[1 + (1.4 \times 10^{-9})\kappa] r_{ij}\zeta_i\zeta_j \tag{65}$$

where

$$r_{ij} = \frac{2r_i r_j}{r_i + r_j}$$

and ζ_i is the zeta potential of ith particles, given by the equation[7]

$$\zeta_i = \left(\frac{2kT}{ze_L}\right)\ln\left(\frac{e^E + 1}{e^E - 1}\right) \tag{66}$$

with

$$E = \kappa\delta + \ln\left(\frac{e^D + 1}{e^D - 1}\right) \quad \text{and} \quad D = \frac{ze_L\psi_{oi}}{2kT} \tag{67}$$

The surface potential, ψ_{oi}, was calculated from the Poisson−Boltzmann equation, assuming that the Debye−Hückel approximation for weakly charged particles and the Gouy−Chapman approximation for highly charged particles are valid[15]

$$\psi_{oi} = \frac{4\pi r_i \sigma_i}{\epsilon(1 + \kappa r_i)} \quad \text{for} \quad \psi_{oi} \le 0.05 \text{ V} \tag{68}$$

$$\psi_{oi} = \frac{2kT}{ze_L}\sinh^{-1}\left(\frac{2\pi z e_L}{\epsilon kT\kappa}\right) \quad \text{for} \quad \psi_{oi} > 0.05 \text{ V} \tag{69}$$

σ_i is the surface charge density, which can be expressed in terms of the total surface particle charge, Q_i, as

$$\sigma_i = Q_i/4\pi {r_i}^2 \tag{70}$$

In the absence of an ionic surfactant, Kiparissides et al.[29] proposed the following expression to relate the total surface charge, Q_i, to the particle radius, r_i

$$Q_i = C_p e_L {r_i}^p \tag{71}$$

where p is an adjustable particle charge parameter. Note that, for $p = 0$, eq 71 will result in a constant surface charge for all particles. On the other hand, for $p = 2$ and $\kappa r_i \gg 1$, eq 68 corresponds to the case of constant surface potential. From electrophoretic mobility measurements, Kiparissides et al.[29] found that the parameter C_p can be expressed as

$$C_p = (1.57 \times 10^{-17})(1.5 \times 10^{-7})^{-p} \tag{72}$$

The Richards et al. model[7] effectively uses a value of $p = 3$, together with a surface charge factor of $\omega = 1$. In the present study, the value of the parameter p was found to be equal to 2.5, resulting in a slow increase in surface potential with particle radius.

Numerical Solution of the Population Balance Equation. Several numerical methods have been proposed in the literature for solving partial integro-differential equations. These include finite-difference methods, the method of moments,[32,33] orthogonal collocation on finite elements,[25,6] geometric discretization methods,[34−36] etc. In the present investigation, a finite-difference discretization method was employed. Prior to the numerical solution of the population balance eq 54, the following logarithmic transformation was applied[29,37]

$$m(w,t) = f(r,t)\frac{dr}{dw} = f(r,t)r \ln J = n(V,t)\frac{dV}{dw} = n(V,t)4\pi r^3 \ln J \tag{73}$$

Accordingly, the whole range of variation of the dimensionless radius w was divided into a suite of equally spaced dimensionless intervals (i.e., w_1, ..., w_N), and eq 54 was approximated by a system of N dif-

ferential equations. w_N was set equal to 1, corresponding to the maximum dimensionless size of the primary particles. The final set of N differential equations obtained from the discretization of the population balance equation can be written as

$$\frac{\mathrm{d}m(w_i,t)}{\mathrm{d}t} + \frac{1}{4\pi(\ln J)r_{\min}^3}\left(\frac{\partial[K(w,t)\, m(w,t)]}{\partial w}\right)_{w_i} = \frac{J^{3w_i}}{2}\int_0^{z_i'}\beta(x_i,z)\, m(x_i,t)\, m(z,t)(J^{3w_i} - J^{3z})^{-1}\,\mathrm{d}z - m(w_i,t)\int_0^1\beta(w_i,z)\, m(z,t)\,\mathrm{d}z \quad i = 1, 2, ..., N \quad (74)$$

where

$$w_i = \frac{\ln(r_i/r_0)}{\ln J}$$

$$J = \frac{r_{\max}}{r_0}$$

$$x_i = \frac{\ln(J^{3w_i} - J^{3z})}{3\ln J} \quad (75)$$

$$z_i' = \frac{\ln(J^{3w_i} - 1)}{3\ln J}$$

$$K = \frac{G_p}{4\pi r^3 \ln J}$$

The corresponding initial and boundary conditions required for the integration of eq 74 are

$$m(w_i,0) = 0.0 \quad \text{for} \quad w_i \geq 0,\ i = 1, ..., N \quad (76)$$

The partial derivative of $m(w,t)$ with respect to w in

$$\frac{\mathrm{d}m(w_1,t)}{\mathrm{d}t} = -m(w_1,t)\int_0^1\beta(w_1,z)\, m(z,t)\,\mathrm{d}z + R_{pg}3\ln J \quad (77)$$

eq 74 was calculated using a two-point backward difference approximation.[35]

The total number of primary particles per unit volume of the reaction medium is given by the zero moment of the number volume density function, $n(V,t)$

$$N_e(t) = \int_{V_0}^{V_N} n(V,t)\,\mathrm{d}V = \int_{w_0}^{w_N} m(w,t)\,\mathrm{d}w = \int_{r_0}^{r_N} f(r,t)\,\mathrm{d}r \quad (78)$$

Accordingly, the average particle radius, r_{pq}, can be calculated from the general equation

$$(r_{pq})^{p-q} = \frac{\int_{r_0}^{r_N} r^p f(r,t)\,\mathrm{d}r}{\int_{r_0}^{r_N} r^q f(r,t)\,\mathrm{d}r} \quad (79)$$

where the indices p and q ($p > q$) can take the values $p = 1, 2, 3, 4, 5$ and $q = 0, 1, 2, 3$. It should be pointed out that common measures of the average particle size include the number-average particle radius ($r_n = r_{10}$), the weight-average particle radius ($r_w = r_{43}$), and the volume-average radius ($r_v = r_{30}$). The broadness of the PSD is characterized by the coefficient S_d/r_n, which is defined as

$$S_d/r_n = [(r_{20})^2 - (r_n)^2]^{1/2}/r_n \quad (80)$$

Table 2. Kinetic Rate Constants and Physical Properties of the Reaction Mixture, at 51 °C

parameter	value	units
k_I[b]	$2.288 \times 10^{16}\exp(-137.9\ \mathrm{kJ\ mol^{-1}}/RT)$	1/s
k_{p11}[a]	10 000	L/(mol·s)
k_{tw11}[a]	3×10^7	L/(mol·s)
k_f[a]	10.98	L/(mol·s)
k_{p12}[a]	10^7	L/(mol·s)
k_{p21}[a]	300	L/(mol·s)
k_{t12}[a]	3×10^7	L/(mol·s)
k_{dVPP}[a]	10^{-4}	1/s
k_m[a]	3×10^{-8}	m/s
D_w[a]	2.5×10^{-9}	m²/s
D_p[a]	2×10^{-11}	m²/s
ρ_T[b]	$1 \times 10^{13}\exp(-105\ \mathrm{kJ\ mol^{-1}}/RT)$	1/s
n[a]	10	–
ρ_m[c]	$(0.9479-1.89) \times 10^{-3}T$ (°C)	kg/m³
ρ_p[c]	1.4	kg/m³
ρ_I[b]	1.98	kg/m³
ρ_s[b]	1.4	kg/m³
α_s'[b]	0.43×10^{-18}	m²/molecule
α_m[b]	0.43×10^{-18}	m²/molecule
ϵ_r[b]	70	–
δ[b]	1.41×10^{-10}	m
p[a]	2.5	
r_{FH}[b]	1.5×10^{-8}	m

[a] Current work. [b] Taken from Richards et al.[7] [c] Taken from Kiparissides et al.[27]

Table 3. Parameters Used in the Diffusion Model[27]

parameter	value	units
V_{fm}	$0.025 + (9.98 \times 10^{-4})(T - T_{gm})$	cm³/cm³
V_{fp}	$0.025 + (5.47 \times 10^{-4})(T - T_{gp})$	cm³/cm³
T_{gm}	70	K
T_{gp}	$87.1 - 0.132(T - 273.15)$	°C
$\hat{V}_m^*$	0.7936	cm³/g
$\hat{V}_p^*$	3.005	cm³/g
ξ	0.375	
γ	2	
δ_d	6×10^{-10}	m
j_c	175	

Results and Discussion

The predictive capabilities of the present model were demonstrated via the successful simulation of experimental measurements of monomer conversion and average particle diameter obtained from a pilot-scale batch VC emulsion polymerization reactor operated over a wide range of oxygen (0−50 ppm) and initiator (250−2000 ppm APS) concentrations. The values of all kinetic, physical, and transport parameters employed in the numerical simulations are reported in Tables 2 and 3. To calculate the VCM conversion the following relationship was employed

$$X = [M_{qe}]/([M_{qe}] + [M_e]) \quad (81)$$

In Figure 2, model predictions are compared with experimental measurements of monomer conversion for different values of the initial oxygen concentration. It should be noted that all reported quantities (i.e., polymerization time, initial oxygen concentration, average particle diameter) have been scaled to corresponding dimensionless values for confidentiality reasons. The sharp increase in the polymerization rate observed at high monomer conversions is due to the well-known phenomenon of the gel effect. As can be seen, the model

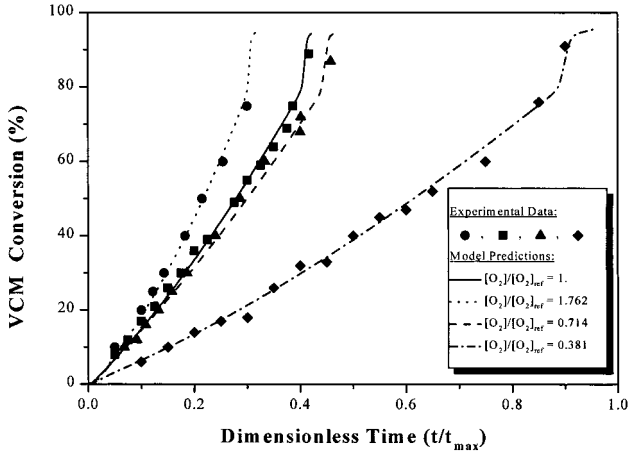

Figure 2. Effect of the initial oxygen concentration on the time history of VCM conversion in a batch emulsion polymerization reactor at 51 °C. Comparison of model predictions with experimental data.

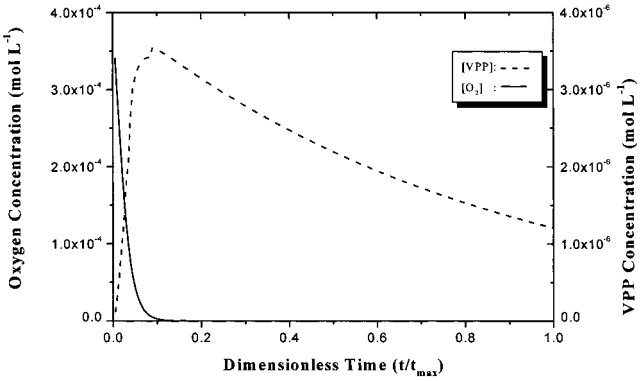

Figure 3. Time variation of the residual oxygen and vinyl polyperoxides concentrations.

predictions for monomer conversion are in excellent agreement with the experimental measurements. In general, it has been observed in the literature that emulsion polymerizations carried out in the presence of oxygen exhibit a decrease in reaction rate.[38] It is important to note that the polymerization rate is largely influenced by the initial oxygen concentration. Thus, as the initial oxygen concentration increases, the polymerization time required to achieve a certain monomer conversion decreases. In all examined cases, the initiator concentration and the polymerization temperature remained constant. It should be noted that particle nucleation was assumed to occur exclusively by the homogeneous mechanism (because of the initial absence of emulsifier).

Figure 3 depicts the time variation of the residual oxygen and vinyl polyperoxide concentrations. As can be observed, the VPP concentration exhibits an initial increase that is followed by a gradual decrease due to the VPP decomposition reaction, eq 4. The time at which the VPP concentration attains its maximum value coincides with the time of disappearance of residual oxygen. From Figure 3, it can be concluded that the formation of VPP radicals occurs during the entire duration of polymerization. As will be shown later on, the VPP decomposition reaction significantly affects the polymerization kinetics and the particle nucleation rate, as well as the stability of latex particles, because it changes the total ionic strength of the aqueous phase through the formation of HCl (see eq 4).

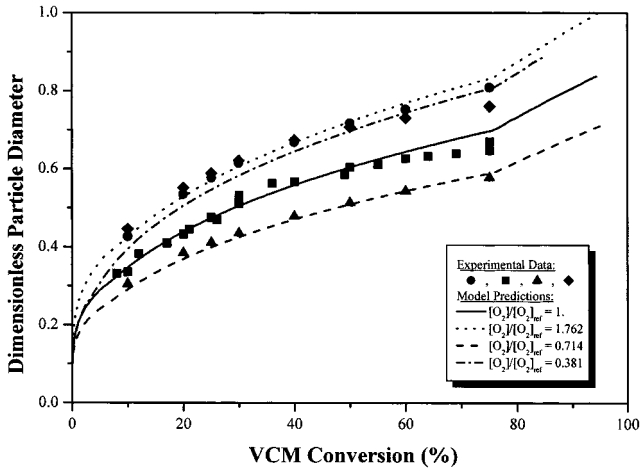

Figure 4. Effect of the initial oxygen concentration on the evolution of the dimensionless average particle diameter. Comparison of model predictions with experimental data.

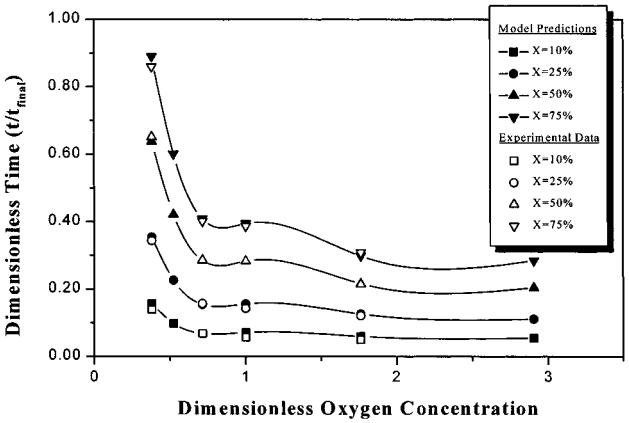

Figure 5. Effect of the initial oxygen concentration on the dimensionless reaction time required to obtain a given VCM conversion. Comparison of model predictions with experimental data.

In Figure 4, the dimensionless particle diameter D_{10}/D_{10max} is plotted with respect to monomer conversion at different values of the dimensionless initial oxygen concentration. Discrete points represent the experimental measurements, whereas model predictions are shown as continuous and broken lines. Apparently, the agreement between the model predictions and the experimental results is excellent.

In Figure 5, the time required to achieve a certain value of monomer conversion is plotted as a function of the initial oxygen concentration at various monomer conversions. Experimental measurements and model predictions are represented by open and solid symbols, respectively. It is clear that the model predictions are in excellent agreement with the experimental measurements. Moreover, the time required to achieve a certain VCM conversion decreases as the initial oxygen concentration increases.

In Figure 6, the dimensionless average particle diameter is plotted as a function of the initial oxygen concentration at various levels of monomer conversion. As can be seen, the ratio D_{10}/D_{10max} exhibits a U-shaped behavior with respect to the initial oxygen concentration. The observed experimental results can be explained by the proposed kinetic mechanism regarding the formation and subsequent decomposition of vinyl polyperoxides (see eqs 1−4). Thus, as the initial oxygen

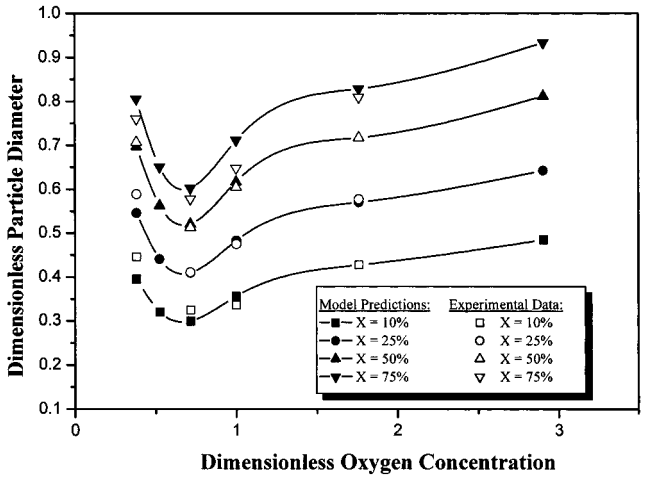

Figure 6. Effect of the initial oxygen concentration on the dimensionless average particle diameter at various VCM conversions. Comparison of model predictions with experimental data.

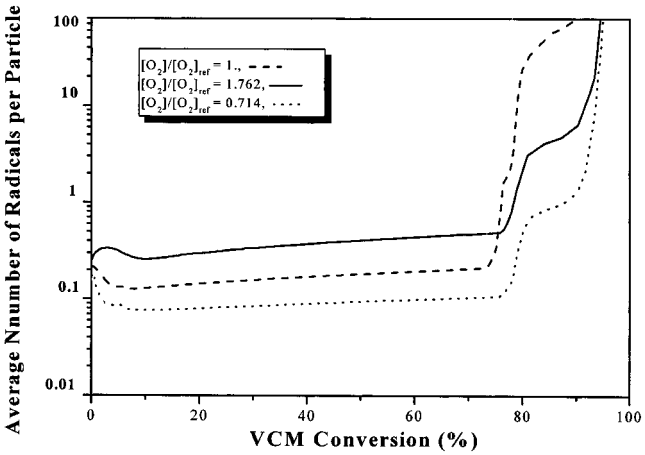

Figure 7. Effect of the initial oxygen concentration on the variation of the average number of radicals per particle with respect to the VCM conversion.

concentration in the batch reactor increases, the concentration of VPPs in the aqueous phase also increases. As a result, the rate of radical production due to VPP decomposition (see eq 4), and, thus, the nucleation rate of primary particles (see eq 57), is increased. This eventually leads to an increase in the total number of particles, along with a concominant decrease in the average particle diameter. However, at higher initial oxygen concentrations, the increased concentration of HCl (formed via the decomposition of VPPs, eq 4) significantly increases the ionic strength of the reaction medium (see eq 64). As a result, particle stability decreases (i.e., the coagulation rate constant, eq 61, increases). Consequently, the number of generated particles decreases, leading to an increase in the average particle diameter. In the latter case, one could expect an overall decrease of the polymerization rate due to the decreased number of generated particles. However, the overall polymerization rate increases, as shown in Figures 2 and 5, because the average number of radicals per particle increases because of the significant contribution of VPP radicals. This is further confirmed by the results of Figure 7, which depicts the effect of the initial oxygen concentration on the average number of radicals per particle, $\bar{n}$. Note that, at very high monomer conversions, $\bar{n}$ can take values as high as 10 as a result of the gel effect.

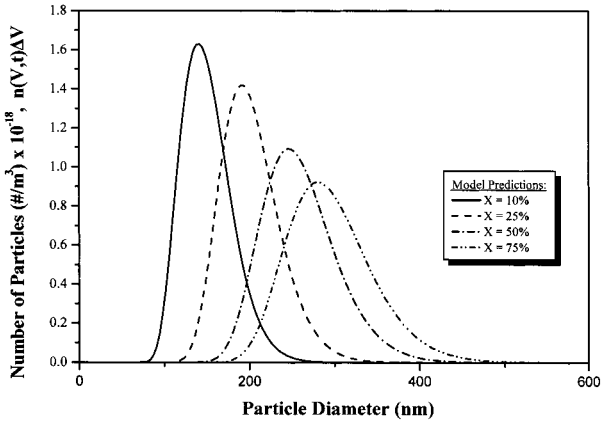

Figure 8. Predicted particle size distributions at different VCM conversions ($[O_2]/[O_2]_{ref} = 1$).

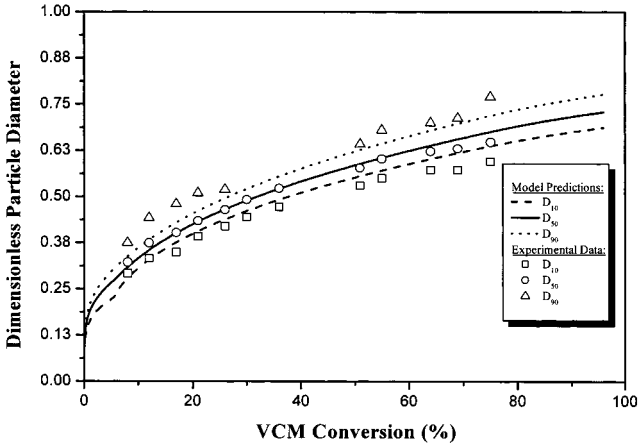

Figure 9. Variation of some characteristic average particle diameters (D_{10}, D_{50}, D_{90}) with respect to VCM conversion. Comparison of model predictions with experimental data ($[O_2]/[O_2]_{ref} = 1$).

Figure 8 depicts the evolution of the particle size distribution with respect to monomer conversion as predicted by the model. It should be noted that the PSD becomes broader as the monomer conversion increases as a result of emulsifier-free particle nucleation conditions. When the emulsifier concentration is below the CMC, particle nucleation proceeds exclusively by the homogeneous mechanism and extends over a longer time period. To provide sufficient stability of the generated latex particles, a predetermined amount of emulsifier was added after an initial nucleation period. Note that the added amount of emulsifier did not exceed the total particle surface area, so that the formation of free micelles, and, thus, the generation of a secondary class of latex particles, could be avoided. In Figure 9, the model predictions are compared with experimental measurements on some average particle diameters (namely, D_{10}, D_{50}, and D_{90}). As can be seen, the agreement between the model predictions and the experimental data is good.

In Figure 10, the effect of the APS concentration on the latex PSD at 75% monomer conversion is illustrated. It can be seen that, as the initial concentration of APS increases, the PSD becomes broader while its mean value shifts to higher values. The results displayed in Figure 10 can be explained by noting that the total ionic strength of the aqueous phase (see eq 64) increases as the APS concentration increases. As a result, the particle coagulation rate increases, which brings about

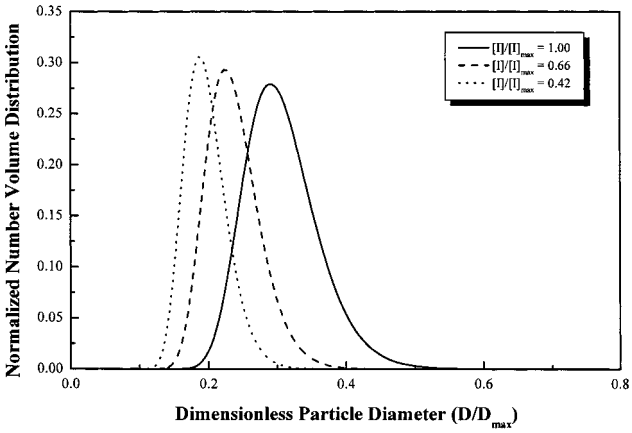

Figure 10. Effect of the initial initiator concentration on the PSD at 75% VCM conversion ($[O_2]/[O_2]_{ref} = 1$).

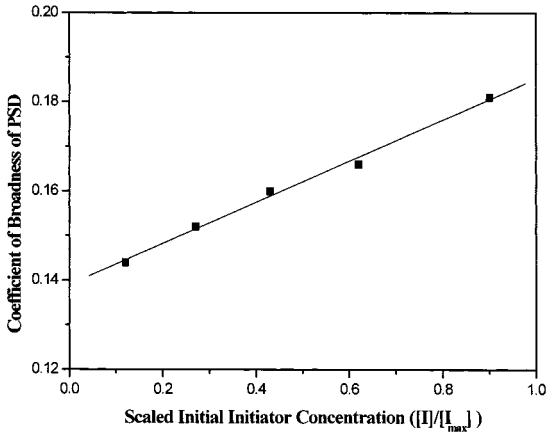

Figure 11. Effect of the initial initiator concentration on the coefficient of broadness of PSD at 75% VCM conversion ($[O_2]/[O_2]_{ref} = 1$).

an increase in the average particle size and leads to the broadening of the PSD.

Finally, in Figure 11, experimental measurements on the broadness coefficient of the PSD (see eq 80) are plotted as a function of the dimensionless initial initiator concentration. It is clear that, as the initial initiator concentration increases, the PSD becomes broader. These results are in full agreement with the experimental observations of Shouldice et al.[13] on the emulsifier-free emulsion polymerization of styrene and the results of Dunn and Chong[14] on the stability and formation of VAc latex particles.

Conclusions

A comprehensive mathematical model for the emulsifier-free emulsion polymerization of VCM in a batch reactor was developed. The effect of the initial oxygen concentration on the polymerization kinetics, the particle nucleation rate, and the particle stability was thoroughly analyzed using a new kinetic mechanism for the formation and decomposition of vinyl polyperoxides. It was shown that the polymerization rate initially increased with the oxygen concentration. On the other hand, the average particle size exhibited a U-shaped behavior with respect to the initial oxygen concentration, which was explained by the combined role of vinyl polyperoxides as a radical generator as well as an ionic strength promoter via the production of HCl. Model predictions were successfully compared with experimental data on VCM conversion and some common particle size averages obtained from an industrial pilot-scale batch reactor operated over a wide range of experimental conditions. The excellent agreement of the theoretical results with the experimental measurements clearly demonstrates the predictive capabilities of the proposed mathematical model.

Acknowledgment

The authors gratefully acknowledge the DGX II of the European Union for supporting this work under the BRITE-EURAM project CT93-0523. The authors also thank Dr. A. Alexopoulos for his constructive comments and suggestions in preparing this article.

Notation

c_t = first-order radical termination constant (1/s)
C_p = parameter in eq 71
D_m = diffusion coefficient of the monomer (m^2/s)
D_p = diffusion coefficient in the polymer phase (m^2/s)
D_w = diffusion coefficient in the aqueous phase (m^2/s)
e_L = electron charge (Cb)
$f(r)$ = density distribution function of particles of radius r (number/m^4)
G_p = volumetric growth rate (m^3/s)
I = initiator concentration (mol/m^3)
I_e = ionic strength (mol/m^3)
j_c = entaglement spacing
j_{cr} = chain length
k = Boltzman constant (J/K)
k_d = radical desorption coefficient (s^{-1})
k_{dVPP} = VPP decomposition rate constant (s^{-1})
k_{ei} = radical entry rate coefficient [m^3/(mol·s)]
k_f = chain transfer to monomer rate constant [m^3/(mol·s)]
k_I = rate constant for thermal decomposition of initiator (s^{-1})
k_{mi} = mass-transfer coefficient for type i radicals entering micelles (m/s)
k_{pii} = propagation rate constant for monomer i [m^3/(mol·s)]
k_{pij} = cross propagation rate constant [m^3/(mol·s)]
k_t = total termination rate constant [m^3/(mol·s)]
k_{td} = diffusion-controlled termination rate constant [m^3/(mol·s)]
$k_{t,res}$ = residual termination rate constant [m^3/(mol·s)]
k_{twii} = termination rate constant for monomer i [m^3/(mol·s)]
k_{twij} = cross termination rate constant [m^3/(mol·s)]
k_o = radical desorption rate constant (s^{-1})
K_{mwp} = water/particle partition coefficient
K_{mdp} = droplet/particle partition coefficient
K_{sol} = solubility of the monomer (g of monomer/ g of water)
M_e = monomer concentration in the emulsion phase (mol/m^3)
M_p = monomer concentration in the polymer phase (mol/m^3)
M_{qe} = monomer concentration in the dead polymer phase (mol/m^3)
$m(w)$ = density distribution function of particles of size w (#/m^3).
M_w = monomer concentration in the aqueous phase (mol/m^3)
MW_m = molecular weight of the monomer (VCM)
n_V = number volume density function of particles of size V (#/m^6)
n = empirical parameter, calculated by fitting to experimental data
$\bar{n}$ = average number of radicals per particle
NAMW = number-average molecular weight of the polymer

N_e = number concentration of particles in the emulsion (#/m^3)
N_A = Avogadro's number (6.023×10^{23} molecules/mol)
p = adjustable particle charge parameter
P_e = dead polymer concentration in the emulsion phase (mol/m^3)
P_w = dead polymer concentration in the aqueous phase (mol/m^3)
P_n = dead polymer concentration in the polymer phase (mol/m^3)
Q_i = total surface charge of particle of size r_i (Cb)
r = radius of particle (m)
r_m = radius of micelle (m)
r_M = effective reaction radius for propagation (m)
r_t = effective reaction radius for termination (m)
r_{FH} = Flory−Huggins radius (m)
r_0 = minimum particle radius (m)
r_{max} = maximum particle radius (m)
R = universal gas constant [1.9872 cal/(mol·K)]
R_d = rate of radical desorption from the particles [mol/(m^3·s)]
R_{ew} = total rate of radical entry into particles [mol/(m^3·s)]
R_{emw} = rate of radical entry into micelles [mol/(m^3·s)]
R_{Iw} = radical production rate in the emulsion phase [mol/(m^3·s)]
R_{pe} = overall polymerization rate in the emulsion phase [mol/(m^3·s)]
R_{pp} = polymerization rate in the polymer phase [mol/(m^3·s)]
R_{pg} = overall particle generation rate [mol/(m^3·s)]
R_{pgm} = micellar nucleation rate [mol/(m^3·s)]
R_{pgh} = homogeneous nucleation rate [mol/(m^3·s)]
R_{pw} = polymerization rate in the aqueous phase [mol/(m^3·s)]
R_{tw} = rate of radical termination in the aqueous phase [mol/(m^3·s)]
$R^{\bullet}_{i,n}$ = radicals terminating in a monomer on an oxygen unit (i = 1, 2) in the aqueous (n = w) or the particulate (n = p) phase
S = surfactant concentration (mol/m^3)
T = temperature (K)
T_g = glass transition temperature (K)
V_i = volume of phase i (m^3)
VPP = concentration of vinyl polyperoxides (mol/m^3)
$\hat{V}^*_i$ = specific critical volume of substance i (m^3/g)
V_{max} = maximum total interaction energy (J)
w = dimensionless particle diameter
W_{ij} = stability ratio between particles of radii r_i and r_j
x = conversion
x_c = critical conversion where droplet phase disappears
Y_w = electrolyte concentration (mol/m^3)
z = ionic valence

Greek Symbols

α_m = surface area occupied by an emulsifier molecule on a micelle (m^2/molecule)
α'_s = surface area occupied by an emulsifier molecule on a particle (m^2/molecule)
β_{ij} = coalescence rate constant between two particles having radii r_i and r_j (m^3/s)
γ = overlap factor
δ_d = average root-mean-square end-to-end distance per square root of the number of monomer units in a chain (m)
δ = Stern layer thickness (m)
ϵ = permittivity of the vacuum [Cb^2/(m·J)]
ϵ_r = relative dielectric constant of the medium
ζ = zeta potential (V)
κ = inverse electric double layer thickness (m^{-1})
μ = viscosity (N s/m^2)
ξ = ratio of the critical molar volume of the jumping unit to the critical molar volume of the polymer jumping unit
ρ_i = density of monomer (i = m), polymer (i = p), initiator (i = I), and surfactant (i = s) (kg/m^3)
ρ = first-order rate constant for radical entry into particles (1/s)
ρ_T = thermal contribution to the radical entry rate (1/s)
σ_i = surface charge density of particle of size r_i (Cb/m^2)
τ = parameter for the calculation of the termination radius
φ_m = volume fraction of monomer in the particulate phase
φ_p = volume fraction of polymer in the particulate phase
ψ_{oi} = surface electric potential of particle of size r_i (V)

Subscripts

e = emulsion phase
CMC = critical micele concentration
f = chain transfer to monomer
I = initiator
m = monomer droplet phase
p = polymer phase
q = dead polymer phase
s = surfactant
sat = saturation
t = termination
w = aqueous phase
0 = initial conditions
1 = radicals ending in a monomer unit
2 = radicals ending in an oxygen unit
w = aqueous phase

Superscripts

* = critical
• = radical species

Literature Cited

(1) Vega, J. R.; Gugliotta, L. M.; Bielsa, R. O.; Brandolini, M. C.; Meira, G. R. Emulsion Copolymerization of AN and Butadiene. Mathematical Model of an Industrial Reactor. *Ind. Eng. Chem. Res.* **1997**, *36*, 1238.

(2) Kishore, K.; Paramasivam, S.; Sandhya, T. E. High-Pressure Kinetics of Polyperoxides. *Macromolecules* **1996**, *29*, 6973.

(3) Bunten, M. J. Vinyl Chloride: Emulsion Polymerization and Plastisols. In *Encyclopedia of Polymer Science and Technology*; Mark, H., Ed.; Wiley: New York, 1994; Vol. 17, p 329.

(4) Zilberman, E. N. The Role of Oxygen in the Polymerization of Vinyl Chloride. *J. Macromol. Sci. Rev.* **1992**, *C32*, 235.

(5) Dube, M. A.; Soares, J. B. P.; Penlidis, A.; Hamielec, A. E. Mathematical Modelling of Multicomponents Chain-Growth Polymerizations in Batch, Semibatch, and Continuous Reactors: A Review. *Ind. Eng. Chem. Res.* **1997**, *36*, 966.

(6) Saldivar, E.; Ray, W. H. Mathematical Modeling of Emulsion Copolymerization Reactors: Experimental Validation and Application to Complex Systems. *Ind. Eng. Chem. Res.* **1997**, *36*, 1322.

(7) Richards, J. R.; Congalidis, J. P.; Gilbert, R. G. Mathematical Modeling of Emulsion Copolymerization Reactors. *J. Appl. Polym. Sci.* **1989**, *37*, 2727.

(8) Storti, G.; Morbidelli, M.; Carra, S. Detailed Modeling of Multicomponent Emulsion Polymerization Systems. In *Computer Applications in Applied Polymer Science II: Automation, Modeling and Simulation*; Provder, T., Ed.; ACS Symposium Series 404; American Chemical Society: Washington, DC, 1989; Chapter 30, p 379.

(9) Forcada, J.; Asua, J. Modeling of Unseeded Emulsion Copolymerization of Styrene and MMA. *J. Polym. Sci. A: Polym. Chem.* **1990**, *28*, 987.

(10) Napper, D. H.; Gilbert, R. G. Polymerization in Emulsions. In *Comprehensive Polymer Science*; Allen, G., Ed.; Pergamon Press: Oxford, U.K., 1988; Vol. IV, p 171.

(11) Dougherty, E. P. The SCOPE dynamic model for emulsion polymerization I. Theory. *J. Appl. Polym. Sci.* **1986**, *32*, 3051.

(12) Min, K. W.; Ray, W. H. On the Mathematical Modeling of Emulsion Polymerization Reactors. *J. Macromol. Sci., Rev. Macromol. Chem.* **1974**, *C11*, 177.

(13) Shouldice, G. T.; Vandezande, G. A.; Rudin, A. Practical Aspects of the Emulsifier-Free Emulsion Polymerization of Styrene. *Eur. Polym. J.* **1994**, *30*, 179.

(14) Dunn, A. S.; Chong, L. C. Application of the Theory of Colloid Stability to the Problem of Particle Formation in Aqueous Solution of VAc. *Br. Polym. J.* **1970**, *2*, 49.

(15) Feeney, P. J.; Napper, D. H.; Gilbert, R. G. Surfactant-Free Emulsion Polymerizations: Predictions of the Coagulative Nucleation Theory. *Macromolecules* **1987**, *20*, 2922.

(16) Chen, Y.-C.; Lee, C.-F.; Chiu, W.-Y. Soapless Emulsion Polymerization of MMA. II. Simulation of Polymer Particle Formation. *J. Appl. Polym. Sci.* **1996**, *61*, 2235.

(17) Min, K. W.; Gostin, H. I. Simulation of Semi-Batch Emulsion Polymerization Reactors for PVC System. *Ind. Eng. Chem. Prod. Res. Dev.* **1979**, *18*, 272.

(18) Tauer, K.; Reinisch, G.; Gazewski, H.; Muller, I. Modeling of Emulsion Polymerization of Vinyl Chloride. *J. Macromol. Sci., Chem.* **1991**, *A28*, 431.

(19) Capek, I. Kinetics of the Free-Radical Emulsion Polymerization of Vinyl Chloride. *Adv. Polym. Sci.* **1995**, *120*, 135.

(20) George, M.; Garton, A. Effect of Oxygen on the Polymerization of Vinyl Chloride. *J. Macrom. Sci., Chem.* **1977**, *A11*, 1389.

(21) Braun, D.; Sonderhof, D. Structural Defects in Poly(vinyl chloride) II. *Eur. Polym. J.* **1982**, *18*, 141.

(22) Ugelstad, J.; Hansen, F. K. Kinetics and Mechanism of Emulsion Polymerization. *Rubber Chem. Technol.* **1976**, *49*, 535.

(23) Nomura, M.; Fujita, K. On the Prediction of the Rate of Emulsion Copolymerization and Copolymer Composition. *Makromol. Chem., Suppl.* **1985**, *10/11*, 25.

(24) Hansen, F. K.; Ugelstad, J. Particle Nucleation in Emulsion Polymerization. I. A Theory for Homogeneous Nucleation. *J. Polym. Sci. A: Polym. Chem.* **1978**, *16*, 1953.

(25) Paquet, D. A., Jr.; Ray, W. H. Tubular Reactors for Emulsion Polymerization: II. Model Comparisons with Experiments. *AIChE J.* **1994**, *40*, 88.

(26) Ugelstad, J.; Moerk, P. C.; Hansen, F. K. Kinetics and Mechanism of Vinyl Chloride Polymerization. *Pure Appl. Chem.* **1981**, *53*, 323.

(27) Kiparissides, C.; Daskalakis, G.; Achilias, D. S.; Sidiropoulou, E. Dynamic Simulation of Industrial PVC Batch Suspension Polymerization Reactors. *Ind. Eng. Chem. Res.* **1997**, *36*, 1253.

(28) Achilias D. S.; Kiparissides, C. Development of a General Mathematical Framework for Modelling Diffusion-Controlled Free Radical Polymerization Reactions. *Macromolecules* **1992**, *25*, 3739.

(29) Kiparissides, C.; Achilias, D. S.; Chatzi, E. Dynamic Simulation of Primary Particle Size Distribution in Vinyl Chloride Polymerization. *J. Appl. Polym. Sci.* **1994**, *54*, 1423.

(30) Casey, B. S.; Morrison, B. R.; Gilbert, R. G. The Role of Aqueous-Phase Kinetics in Emulsion Polymerizations. *Prog. Polym. Sci.* **1993**, *18*, 1041.

(31) Reerink, H.; Overbreek, J. Th. G. The Rate of Coagulation as a Measure of the Stability of Silver Iodide Sols. *Discuss. Faraday Soc.* **1954**, *18*, 74.

(32) Min, K. W.; Ray, W. H. The Computer Simulation of Batch Emulsion Polymerization Reactors through a Detailed Mathematical Model. *J. Appl. Polym. Sci.* **1978**, *22*, 89.

(33) Storti, G.; Carra, S.; Morbidelli, M.; Vita, G. Kinetics of Multimonomer Emulsion Polymerization. The Pseudo-Homopolymerization Approach. *J. Appl. Polym. Sci.* **1989**, *37*, 2443.

(34) Hounslow, M. J.; Ryall, R. L.; Marshall, V. R. A Discretized Population Balance for Nucleation, Growth and Aggregation. *AIChE J.* **1988**, *34*, 1821.

(35) Muhr, H.; David, R.; Villermaux, J.; Jezequel, P. H. Crystallization and Precipitation Engineering VI. *Chem. Eng. Sci.* **1996**, *51*, 309.

(36) Kumar, S.; Ramkrishna, D. On the Solution of Population Balance Equations by Discretization I. *Chem. Eng. Sci.* **1996**, *51*, 1311.

(37) Gelbard F.; Seinfeld, J. H. Numerical Solution of the Dynamic Equation for Particulate Systems. *J. Comput. Phys.* **1978**, *28*, 357.

(38) de Arbina, L. L.; Gugliotta, L. M.; Barandiaran, M. J.; Asua, J. M. Effect of oxygen on emulsion polymerisation kinetics: A study by reaction calorimetry. *Polymer* **1998**, *39*, 4047.

Received for review November 13, 2001
Revised manuscript received April 4, 2002
Accepted April 8, 2002

IE010928F